IJEP 45 (11) : 1016-1023 (2025) (ISSN : 0253-7141)

Constructive and Ecological Energy Storage - A Carbon Coated TiO_2 Nano Composite Anode for Sodium Ion Battery Derived from *Prosopis juliflora* Plant Wood

Pavithra Kamatchisundaram and Meyappan Revathi*

Vels Institute of Science, Technology and Advanced Studies, Department of Chemistry, Pallavaram, Chennai - 600 117, Tamil Nadu, India

**Corresponding author, Email: mrev80@gmail.com; dr.revathichem.sbs@vistas.ac.in*

Sodium-ion batteries (SIBs) are proposed as cost-effective and environmentally friendly options for electric mobility and grid storage applications. In this context, hard carbon is a promising anode material for SIBs because of its electrochemical performance. Recently, biowaste resources have attracted significant attention among many hard carbon precursors due to their affordability, availability and sustainability. Here, we report the synthesis of hard carbon from *Prosopis juliflora* plant biowaste, which is a cost-effective and efficient strategy for developing active carbon-based materials for Na-ion batteries. The produced carbon was coated onto TiO_2 nanoparticles using a straightforward ball milling process. The resulting C-TiO_2 nano-composite was tested as an anode material for sodium-ion batteries. It delivered an initial discharge capacity of 418 mAh/g when cycled between 0.2-3.0 V. The C-TiO_2 composite electrode shows good capacity retention at low discharge voltages. X-ray diffraction patterns confirm the formation of the C-TiO_2 composite, while Raman spectra verify its defect-rich graphitic structure. Surface micrographs clearly indicate highly permeable carbon coating extensively covering the surface of TiO_2 nanoparticles.

KEYWORDS

Biomass carbon, TiO_2, *Prosopis juliflora*, Composite anode, Sodium-ion battery, Eco-friendly

1. INTRODUCTION

The demand for high-power rechargeable batteries is increasing due to the rapid growth of many portable electronic devices and electric vehicles. Limited lithium resources are driving the search for alternative technologies. Currently, sodium-ion batteries (SIBs) have gained significant attention and are considered a potential alternative to lithium-ion batteries (LIBs). The abundant sodium resources with similar electrochemical properties to lithium have accelerated research into Na-ion batteries [1,2]. However, there are currently no suitable electrodes for sodium-ion batteries that can make the technology practical. The large ionic radius of Na^+ (1.02 A) is one of the main challenges [3]. Lithium-ion batteries succeed with graphite anodes because of the stable formation of Li-C bonds in carbon-based materials. Many studies have confirmed that conventional graphite is not suitable for sodium-ion batteries due to the lack of stable sodium-carbon (Na-C) compounds. Furthermore, recent research exploring Na^+ intercalation with graphite has examined the movement of sodium ions with electrolyte solvent and graphite anodes, often resulting in unstable Na-C formation [4]. Various non-graphitic carbon materials have been tested as sodium anodes [5-8]. Low-potential intercalation-type anodes, such as $Na_2Ti_3O_7$, based on insertion mechanisms, have been reported by Onoh *et al.* (2024) and Senguttuvan *et al.* (2011), showing reasonable capacities [9,10].

Recently, titanium dioxide (TiO_2) has emerged as a promising anode material for Na-ion batteries due to its high structural stability, non-toxicity and low-cost. It also provides favourable pathways within its structure for sodium ion accommodation during cycling. The Ti^{4+}/Ti^{3+} redox couple is expected to deliver high capacities [11-13]. Coating TiO_2 with carbon has been shown to enhance Na^+ diffusion during intercalation because it can prevent nanoparticle aggregation during charge and discharge cycles. Consequently, Liu *et al.* (2022) reported a carbon-TiO_2 composite with improved electrochemical performance and Ge *et al.* (2015) observed notable capacity retention with carbon-coated TiO_2 particles

compared to pure TiO_2 [14,15]. Dias *et al.* (2022) demonstrated that graphene/metal oxide composites improve electrochemical properties, such as high capacity, rate capability and cycling stability [16]. Doped graphene is considered a promising anode for high-power lithium-ion batteries due to its high charge/discharge rates, with mesoporous carbon providing easy pathways for ion migration and graphitic structure enabling low-resistance electron transfer [17,18]. Additionally, hard carbon anodes show good sodium storage capabilities, with discharge capacities around 200–300 mAh/g [19]. Stevens and Dahn (2000) confirmed that sodium ions exhibit free kinetics in hard carbon [20]. Therefore, TiO_2 nanoparticles combined with carbon can enhance electrochemical performance in sodium batteries. Carbon and metal oxides, often derived from various biowastes due to their low-cost and ease of processing, are widely used as electrode materials in batteries and supercapacitors [21-24].

In this study, we derived carbon from the bark of the *Prosopis juliflora* plant because it has high lignocellulose content, offering high porosity and surface area; it is abundant in India, which helps address water depletion, soil infertility and ecosystem disruption caused by its invasive spread and it is inexpensive and convenient to process [25]. This porous carbon-TiO_2 composite was tested as an anode material for sodium-ion batteries [26]. The electrode was prepared via a simple process using an abundant, non-toxic waste precursor, making it economical and environmentally friendly for low-cost energy storage applications.

2. MATERIAL AND METHOD

The wood of *Prosopis juliflora* was collected, cut into small pieces and dried at 110 °C for 3-4 hr. The dried material was soaked in concentrated sulphuric acid for 24 hr. After 24 hr, the product was washed with excess water to remove free acids, dried again at 110°C and then thermally activated at 800°C for 0.5 hr in a muffle furnace. The material was then cooled to room temperature, ground into a powder, sieved and stored in an airtight container. Subsequently, the derived carbon was ball milled at 250 rpm for 2 hr with purchased bare TiO_2 (15:85 of C-TiO_2 ratio) to obtain the C-TiO_2 composite material [27,28].

2.1 Material characterizations

The XRD patterns of the prepared C-TiO_2 composite were obtained using a PANalytical X'pert-Pro X-ray diffractometer with Cu Kα radiation (1.5406 A). BET analysis was performed with Nova-Quantachrome instruments using the volumetric method. Raman measurements were carried out using an Olympus Raman spectrometer. A chemical state analysis of the C-TiO_2 samples was performed with a PHI Versa Probe III XPS microprobe equipped with a flexible monatomic Ar ion beam. The surface morphology and microstructure of the composite were characterized by FE-SEM QUANTA 200 FEG. HR-TEM images were obtained using a JEM 2100F JEOL HR-TEM. All electrochemical measurements were conducted with a BCS-815/electrochemical analyzer (Bio-Logic, France) in a 2032-type coin cell using PVdF-SiO_2 composite as the separator with Na metal as the counter electrode and 1 M NaPF6 in PC as the electrolyte [29]. The C-TiO_2 composite electrodes were fabricated by mixing 80 wt% active material, (Super P) (99.99%, Alfa Aesar), 10 wt% binder poly (vinylidene fluoride) (PVdF, Sigma-Aldrich) and solvent N-methyl-2-pyrrolidone (NMP). The slurry was coated onto an Al foil current collector and dried in a vacuum oven at 80°C for 18 hr. All cells were assembled in Ar-filled glove box (Lab 2000-Etelux) with moisture content below 0.1 ppm. Galvanostatic charge/discharge tests were performed within a voltage range of 0.2–3.0 V (vs Na/Na^+). Cyclic voltammetry (CV) was conducted at 0.1 mV/s and electrochemical impedance spectroscopy (EIS) measurements were performed; the results are discussed [30,31].

3. RESULT AND DISCUSSION

The structures of the materials were analyzed using X-ray diffraction and all the diffraction patterns of the derived carbon, TiO_2 and C-TiO_2 composite are shown in figure 1a. All observed diffraction peaks (TiO_2) can be indexed to the anatase TiO_2 (JCPDS 21-1272). Here, among all the polymorphs of TiO_2 (anatase, rutile, brookite), the anatase form was suitable for larger sodium insertion due to its open layer structure [14,26]. It is observed that after coating the derived carbon on TiO_2, the intensity of TiO_2 diffraction peaks was drastically reduced, which may be due to the amorphous nature of the carbon. To describe the defects and order of the derived carbon, Raman spectroscopy was performed and presented in figure 1b. The typical peak at 1348 cm^{-1} in the Raman spectrum resembles the D band of carbon, indicating the disordered nature of the derived carbon. The peak at 1580 cm^{-1} revealed the (graphitic) G band of carbon, representing presence of graphitic character in the derived carbon. The (ID/IG ratio) of D and G bands in the Raman spectra helps estimate the defects in graphite-based materials. A higher ratio indicates more defects in the carbon structure, with the calculated ID/IG ratio being around 1.02. To evaluate

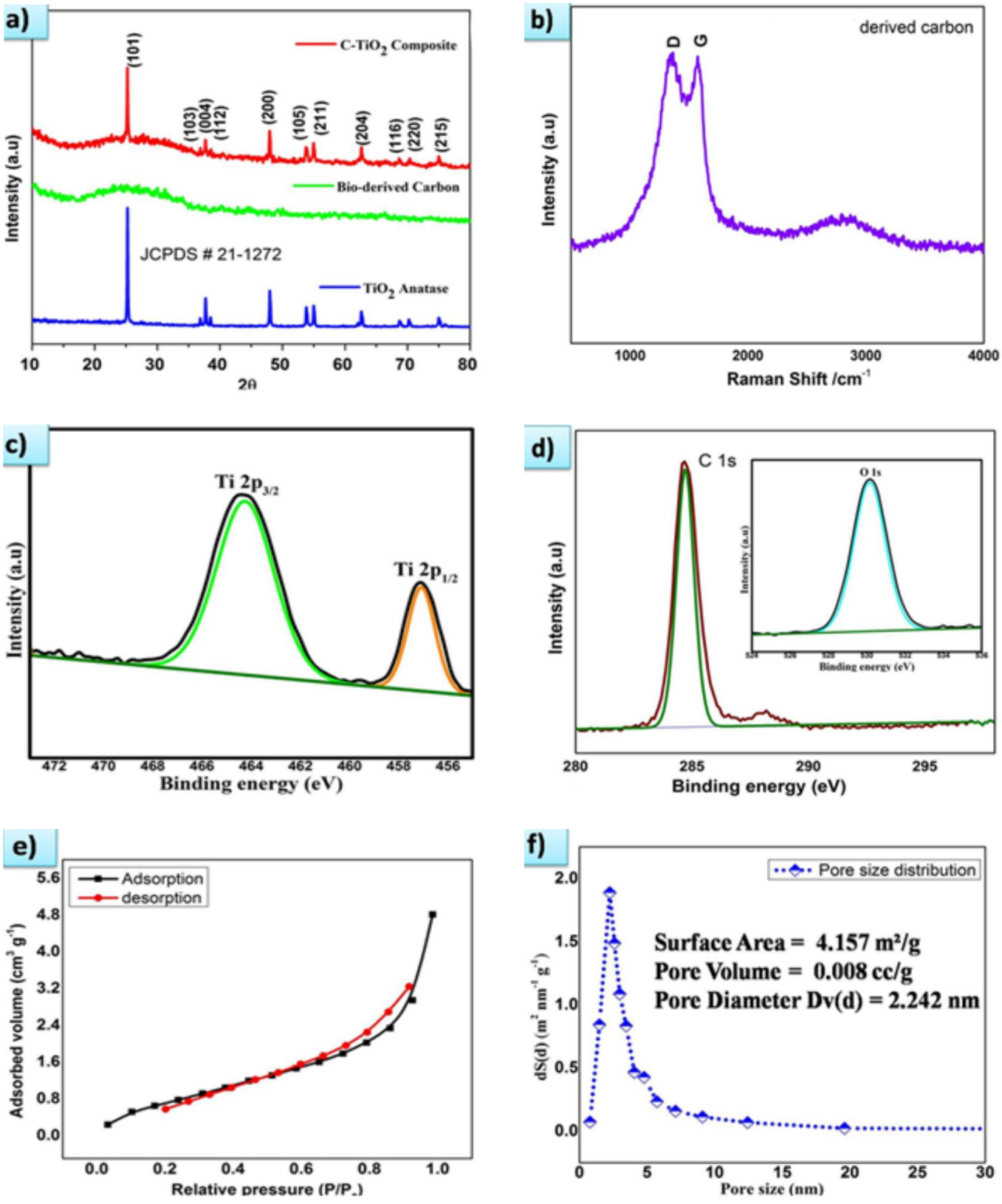

Figure 1. *(a) X-ray diffraction pattern of derived carbon, TiO_2 and C-TiO_2 composite; (b) Raman spectra of derived carbon; (c) XPS spectra of Ti, (d) XPS spectra of C and O, (e) N_2 adsorption/desorption plot of derived carbon and (f) pore size distribution of permeable carbon*

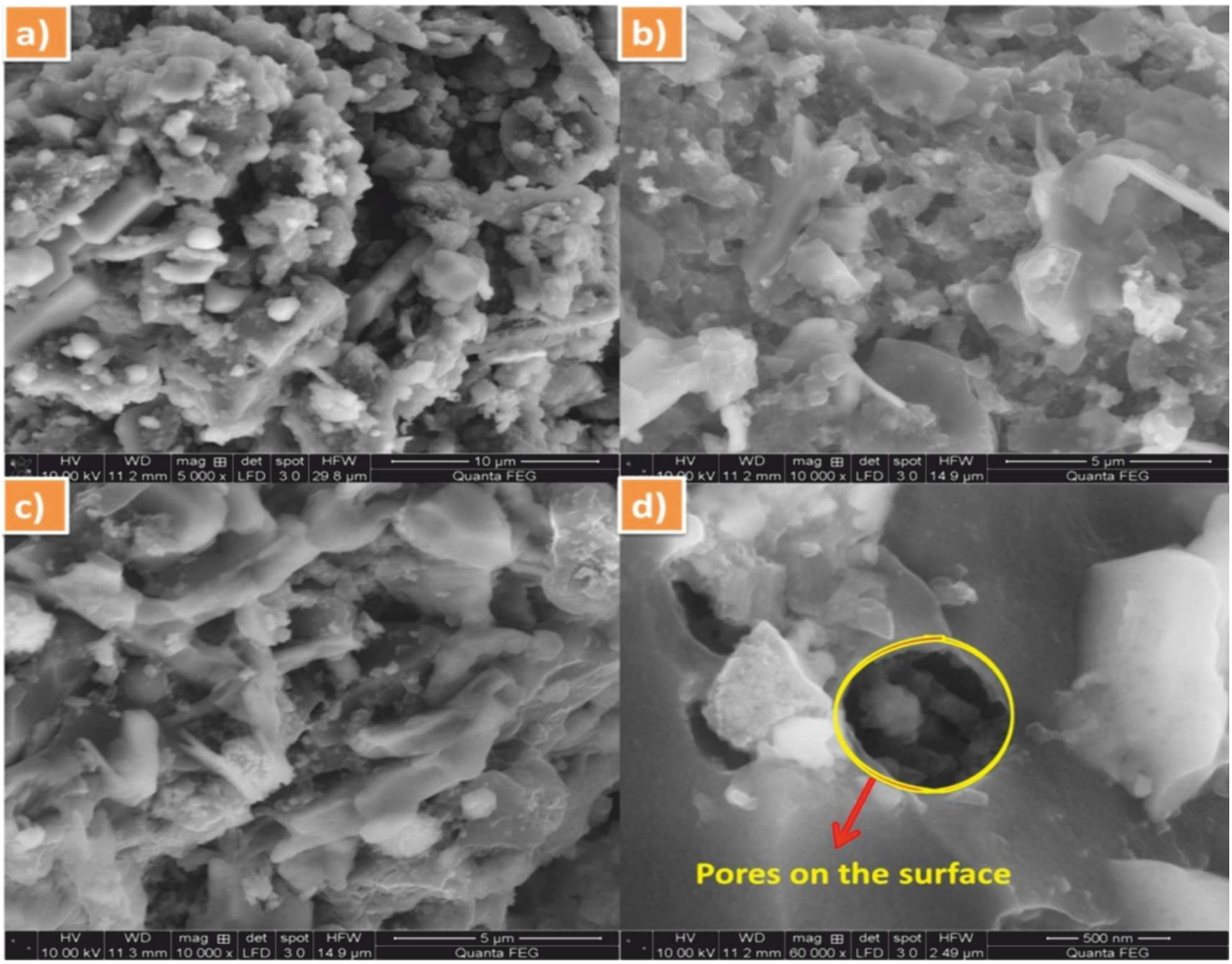

Figure 2. *SEM micrographs of derived carbon from Prosopis juliflora plant at different magnifications: (a) flower-like surface structure, (b-c) exfoliated layer sheets with similar morphology and (d) pores on the derived carbon*

the surface chemical state of the C-TiO_2 composite, X-ray photoelectron spectroscopy was performed (Figure 1c,d). The Ti $2p^{3/2}$ and $2p^{1/2}$ peaks appeared at binding energies of 464 eV and 458 eV, respectively. Figure 1d shows the C1s spectra of the composite, where the peak at 283.6 eV indicates sp^2 hybridization of the C-C bond. The O1s peak at 530.2 eV is assigned to the binding energy characteristic of O1s in TiO_2 (Figure 1d) [32,33]. To assess the permeable nature of the C-TiO_2 composite surface, BET analysis was carried out and the N_2 adsorption-desorption isotherm was obtained (Figure 1e,f). The isotherm shows a hysteresis loop between 0.2-1 in relative pressure (P/P0), indicating a highly porous structure of the materials. This is corroborated by the pore size distribution plot which shows the pore sizes of the TiO_2/C distributed around 1-3 nm (Figure 1f).

The surface microstructure was analyzed using FE-SEM with different magnifications and the micrographs are shown in figure 2. The derived carbon exhibits randomly distributed pores on the surface (Figure 2b,c). A single pore was observed on the surface at a scale of 500 nm in figure 2d, which demonstrates the porous nature of the derived carbon. Since it is a key factor for enhancing the accommodation of high ionic radii sodium atoms during cycling, it is strongly believed that the material can be used efficiently in practical applications. The HR-TEM images of the as-prepared C-TiO_2 composite are shown in figure 3. From the micrographs, it is observed that the particles range from 60-100 nm. The carbon-overlapped TiO_2 particle is shown in figure 3e, the coating width of carbon on TiO_2 is approximately 3 nm. The SAED pattern reveals polycrystalline nature of as-prepared sample. The electrochemical performance

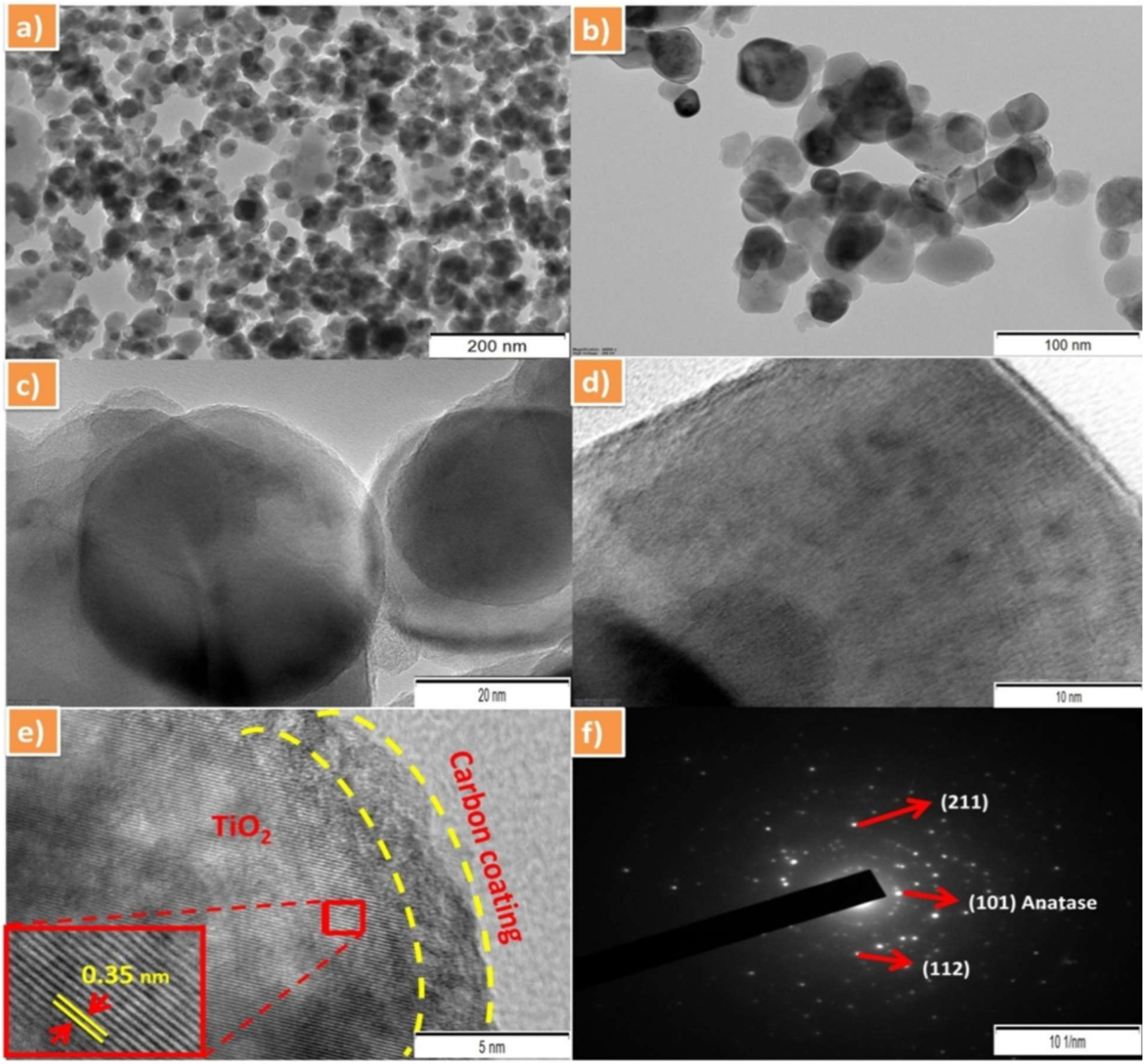

Figure 3. *(a-b) HR-TEM images of carbon-coated C-TiO_2 nanoparticles, (c-d) single nanoparticle of the prepared C-TiO_2 composite, (e) carbon-coated layer on the surface of TiO_2 particle with layered lattice fringes and (f) SAED pattern of the prepared composite*

of the as-prepared composite material was analyzed by galvanostatic charge/discharge.

The C-TiO_2 composite material delivered an initial discharge capacity of 418 mAh/g with 66% coulombic efficiency when cycled between 0.2-3.0 V at 0.05 C (Figure 4a). According to Wu *et al.* (2013), the high initial capacity of TiO_2 anodes is due to the irreversible processes of Na^+ intercalation into TiO_2, which also leads to the significant irreversible capacity during early cycles [34]. The discharge curves of prepared C-TiO_2 composite resembled those reported by Ge *et al.* (2015) [15]. The material exhibits 98% efficiency after 100 cycles, with a capacity of 98 mAh/g (Figure 4b). The rate performance analysis of C-TiO_2 composite anode is shown in figure 4c. The prepared C-TiO_2 anode material exhibits considerable reversible capacity when operated at various C rates (0.05, 0.5, 1, 2 and 5 C). Even at a high current rate (5 C), material maintains a reversible capacity of 94 mAh/g. When returning to the lower rate of 1 C immediately afterwards, it recovers to approximately ~180 mAh/g, indicating excellent tol-

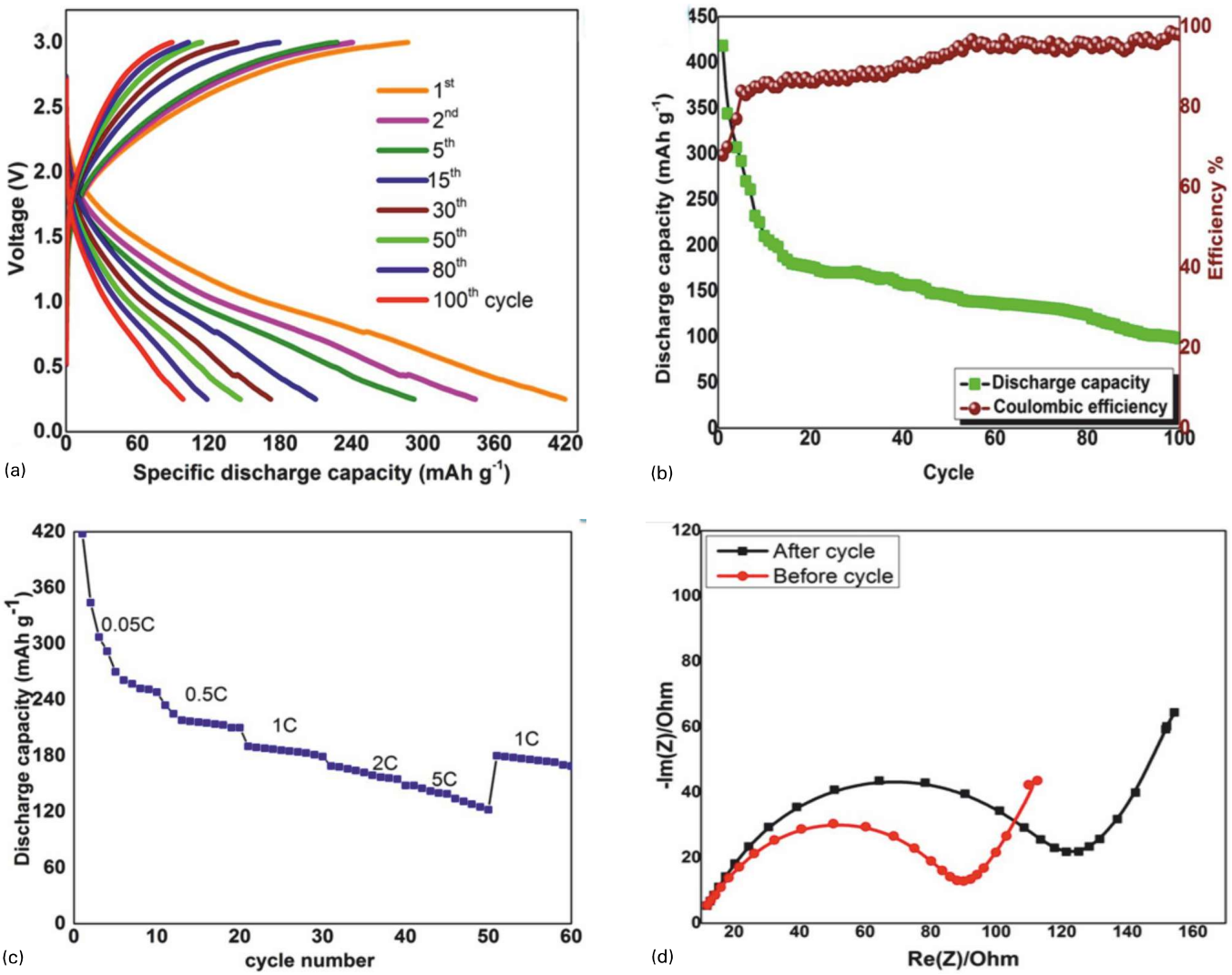

Figure 4. *(a) Charge/discharge plot of C-TiO_2 anode vs Na^+/Na0 between 0.25-3.0 V, (b) capacity delivery and coulombic efficiency over 100 cycles at 0.05 C rate, (c) rate performance of C-TiO_2 anode at various current rates and (d) impedance spectra of the cell before and after cycling*

erance to rapid Na ion insertion and extraction across different C rates.

To investigate the interfacial activity of the composite, impedance spectroscopy (EIS) was performed; this analysis is a useful tool for examining ion kinetics [35,36]. The Nyquist plots were obtained for the C-TiO_2 anode both before and after cycling, spanning a frequency range from 10 kHz to 10 Hz (Figure 4d). The impedance spectra show the diffusion resistance of Na^+ through the SEI in the high-frequency semicircle and the charge transfer resistance (Rct) at interface between the C-TiO_2 anode and electrolyte is indicated by the semicircle in the medium-frequency range [15,37]. The sloped line in the low-frequency region reflects Na^+ diffusion within the cell. The materials follow the same trend in EIS analysis even after cycling, demonstrating the excellent performance of C-TiO_2 composite material for sodium batteries. Wang *et al.* (2018) reported reed straw-derived hard carbon as an anode material for sodium-ion batteries, with an initial capacity of 372 mAh/g and 77% coulombic efficiency [38]. Recent studies have shown that pure TiO_2 nanotubes used as anodes for sodium-ion batteries deliver around 150 mAh/g [39]. In this work on the C/TiO_2 composite anode for sodium-ion batteries, we report a capacity delivery of 418 mAh/g. The electrochemical performance of the C-TiO_2 anode material can be attributed to the following factors. The porous structure of the derived carbon ensures durable contact between the electrode and electrolyte interfaces, facilitating rapid transport of sodium ions and electrons despite volume

expansion during the intercalation process. The electronic conductivity of the electrode is enhanced by the carbon coating. The porous surface structure can ensure fast kinetics for sodium ion transport.

4. CONCLUSION

In this work, we successfully derived porous carbon from biomass through a simple heating process and the composite C-TiO_2 materials were synthesized by mechanical ball-milling as anodes for sodium-ion batteries. We studied the effect of the carbon coating on bare TiO_2 using physical and electrochemical analysis. The C-TiO_2 composite anode material has a smaller particle size. It delivered an initial capacity of around 418 mAh/g with 98% coulombic efficiency. The C-TiO_2 composite electrode showed the best cyclic and rate performance at different current rates, even after 100 cycles, maintaining 98 mAh/g. These excellent electrochemical properties are attributed to the uniformly coated carbon layer on bare TiO_2. Based on the results, the carbon-coated C-TiO_2 composite material could be a safe, low-cost anode option for sodium-ion batteries.

REFERENCES

1. Wu, Y., *et al.* 2024. Recent progress in sodium-ion batteries: Advanced materials, reaction mechanisms and energy applications. *Electrochem. Energy Reviews.* 7(1): 17.
2. Yazie, N., *et al.* 2023. Development of polymer blend electrolytes for battery systems: Recent progress, challenges and future outlook. *Mater. Renew. Sustain. Energy.* 12(2): 73-94.
3. Wuttig, M., *et al.* 2023. Revisiting the nature of chemical bonding in chalcogenides to explain and design their properties. *Adv. Mater.,* 35(20): 2208485.
4. Yoon, G. 2022. Conditions for reversible Na intercalation in graphite. **In** Theoretical study on graphite and lithium metal as anode materials for next-generation rechargeable batteries. Springer Nature, Singapore. pp 29-45.
5. Chen, X., *et al.* 2022. An overall understanding of sodium storage behaviours in hard carbons by an adsorption intercalation/filling hybrid mechanism. *Adv. Energy Mater.,* 12(24): 2200886.
6. Thomas, P., J. Ghanbaja and D. Billaud. 1999. Electrochemical insertion of sodium in pitch-based carbon fibres in comparison with graphite in $NaClO_4$–ethylene carbonate electrolyte. *Electrochimica Acta*. 45(3): 423-430.
7. Qiu, R., *et al.* 2024. Performance degradation mechanisms and mitigation strategies of hard carbon anode and solid electrolyte interface for sodium-ion battery. *Nano Energy.* 28: 109920.
8. Or, T., *et al.* 2022. Recent progress in surface coatings for sodium-ion battery electrode materials. *Electrochem. Energy Reviews.* 5(1): 20.
9. Onoh, E.U., *et al.* 2024. Experimental and theoretical investigation of high-performance green-synthesized $NaTiO_2$/AC nanocomposite as high-capacity electrodes for next-generation sodium-ion capacitors. *J. Mater. Sci.,* 59(40): 19210-19227.
10. Senguttuvan, P., *et al.* 2011. $Na_2Ti_3O_7$: Lowest voltage ever reported oxide insertion electrode for sodium ion batteries. *Chem. Mater.*, 23(18): 4109-4111.
11. Lunell, S., *et al.* 1997. Li and Na diffusion in TiO_2 from quantum chemical theory vs electrochemical experiment. *J. American Chem. Soc.,* 119 (31): 7374-7380.
12. Wang, J. 2023. Sawdust-derived hard carbon as a high-performance anode for sodium-ion batteries. *Ionics.* 29(6): 2311-2318.
13. Su, D., S. Dou and G. Wang. 2015. Anatase TiO_2: Better anode material than amorphous and rutile phases of TiO_2 for Na-ion batteries. *Chem. Mater.* 27(17): 6022-6029.
14. Liu, J. 2022. Facile synthesis of high quality hard carbon anode from eucalyptus wood for sodium-ion batteries. *Chem. Papers.* 76(12): 7465-7473.
15. Ge, Y., *et al.* 2015. High cyclability of carbon-coated TiO_2 nanoparticles as anode for sodium-ion batteries. *Electrochimica Acta*. 157: 142-148.
16. Dias, A., *et al.* 2022. N-graphene-metal-oxide (sulphide) hybrid nanostructures: Single-step plasma-enabled approach for energy storage applications. *Chem. Eng. J.,* 430: 133153.
17. Bi, J., *et al.* 2023. On the road to the frontiers of lithiumion batteries: A review and outlook of graphene anodes. *Adv. Mater.,* 35(16): 2210734.
18. Chang, Y., *et al.* 2022. Labyrinth maze-like long travel-reduction of sulphur and polysulphides in micropores of a spherical honeycomb carbon to greatly confine shuttle effects in lithium-sulphur batteries. *Mater. Reports: Energy.* 2(4): 100159.
19. Wang, Z., *et al.* 2013. Functionalized N-doped interconnected carbon nanofibers as an anode material for sodium-ion storage with excellent performance. *Carbon*. 55: 328-334.
20. Stevens, D.A. and J.R. Dahn. 2000. High capacity anode materials for rechargeable sodium ion batteries. *J. Electrochem. Soc.*, 147(4): 1271.

21. Oyedotun, K.O., *et al.* 2023. Advances in supercapacitor development: Materials, processes and applications. *J. Electronic Mater.,* 52(1): 96-129.
22. Acharya, D., *et al.* 2023. Double-phase engineering of cobalt sulphide/oxyhydroxide on metal-organic frameworks derived iron carbide-integrated porous carbon nanofibers for asymmetric supercapacitors. *Adv. Composites Hybrid Mater.,* 6(5): 179.
23. Merlet, C., *et al.* 2012. On the molecular origin of supercapacitance in nanoporous carbon electrodes. *Nature Mater.*, 11(4): 306-310.
24. Yin, Y., *et al.* 2023. Recent progress and future directions of biomass-derived hierarchical porous carbon: Designing, preparation and supercapacitor applications. *Energy Fuels.* 37(5): 3523-3554.
25. Theriselvam, K., *et al.* 2024. Effect of biochar extracted from *Prosopis juliflora* flora plant with paraffin wax and its performance on leakage, thermal storage and thermal properties. *Interactions.* 245(1): 169.
26. Devarajan, J. and P. Arumugam. 2022. Boron-doped activated carbon from the stems of *Prosopis juliflora* as an effective electrode material in symmetric supercapacitors. *J. Mater. Sci. Mater. Electronics*. 33(22): 17469-17482.
27. Raj, F.R.M.S., *et al.* 2022. Sustainable development through restoration of *Prosopis juliflora* species into activated carbon as electrode material for supercapacitors. *Diamond Related Mater.,* 121: 108767.
28. Baghel, P., A. K. Sakhiya and P. Kaushal 2022. Influence of temperature on slow pyrolysis of *Prosopis juliflora*: An experimental and thermodynamic approach. *Renew. Energy*. 185: 538-551.
29. Arjunan, P., *et al.* 2020. Superior ionic transferring polymer with silicon dioxide composite membrane via phase inversion method designed for high performance sodium-ion battery. *Polymers*. 12(2): 405.
30. Xu, Y., *et al.* 2013. Nanocrystalline anatase TiO_2: A new anode material for rechargeable sodium ion batteries. *Chem. Communications*. 49(79): 8973-8975.
31. Wu, L., *et al.* 2015. Unfolding the mechanism of sodium insertion in anatase TiO_2 nanoparticles. *Adv. Energy Mater.*, 5(2): 1401142.
32. Zhu, L., *et al.* 2017. Ligand-free rutile and anatase TiO_2 nanocrystals as electron extraction layers for high performance inverted polymer solar cells. *RSC Adv.,* 7(33): 20084-20092.
33. Jerng, S.K., *et al.* 2011. Graphitic carbon growth on crystalline and amorphous oxide substrates using molecular beam epitaxy. *Nanoscale Res. Letters.* 6(1): 565.
34. Wu, W. Q., *et al.* 2013. Hydrothermal fabrication of hierarchically anatase TiO_2 nanowire arrays on FTO glass for dye-sensitized solar cells. *Sci. Reports.* 3(1): 1352.
35. Aurbach, D., *et al.* 1999. Capacity fading of $Li_xMn_2O_4$ spinel electrodes studied by XRD and electroanalytical techniques. *J. Power Sources.* 81: 472-479.
36. Liu, J., *et al.* 2014. Facile synthesis of carbon encapsulated $Li_4Ti_5O_{12}$@C hollow microspheres as superior anode materials for Li-ion batteries. *European J. Inorganic Chem.,* 2014(12): 2073-2079.
37. Liu, J., *et al.* 2014. Iron fluoride hollow porous microspheres: Facile solution phase synthesis and their application for Li-ion battery cathodes. *Chem. European J.*, 20(19): 5815-5820.
38. Wang, J., *et al.* 2018. Facile hydrothermal treatment route of reed straw-derived hard carbon for high performance sodium ion battery. *Electrochimica Acta*. 291: 188-196.
39. Liang, S., *et al.* 2022. Bronze phase TiO_2 as anode materials in lithium and sodium ion batteries. *Adv. Functional Mater.,* 32(25): 2201675.